N71-22154 NASA CR-117756

MARINER 6 and 7 ULTRAVIOLET SPECTROMETER EXPERIMENT: UPPER ATMOSPHERE DATA

C. A. Barth
C. W. Hord
J. B. Pearce
K. K. Kelly
G. P. Anderson
A. I. Stewart

Department of Astro-Geophysics and
Laboratory for Atmospheric and Space Physics
University of Colorado, Boulder, 80302

ABSTRACT

Mariner 6 and 7 observations of the Mars upper atmosphere show the ultraviolet emission spectrum to consist of the CO_2^+ A-X and B-X bands, the CO a-X and A-X bands, the CO^+ B-X bands, the CI 1561 and 1657 Å lines, the OI 1304, 1356, and 2972 Å lines, and the HI 1216 Å line. Laboratory measurements and theoretical calculations show that the CO_2^+ band systems are produced by the combination of photoionization excitation of CO_2 and fluorescent scattering of CO_2^+. An analysis of the vibrational populations of the CO Cameron bands shows that they may be produced from photon or electron dissociative excitation of CO_2. The vibrational distribution of the CO fourth positive bands is the same in the Mars spectrum as in a laboratory CO_2 dissociative excitation spectrum except for those bands that are self-absorbed by CO in the Mars atmosphere. Since the CI 1561 Å and 1657 Å lines and the OI 1356 Å and 2972 Å lines may be produced in the laboratory by CO_2 dissociative excitation processes, these are the most likely sources

in the Mars atmosphere. The altitude distribution of all of the emissions, except the HI 1216 Å and OI 1304 Å lines and part of the CO_2^+ A-X bands, is the same and the scale heights indicate a cold, predominantly CO_2 atmosphere. The OI 1304 Å line emission extends to much higher altitudes than the CO_2 emissions showing that atomic oxygen is present. Its profile suggests that it is excited by more than one mechanism. Fluorescent scattering of the CO_2^+ A-X and B-X bands indicates the presence of CO_2^+, but CO_2^+ is not necessarily an abundant ion. Lyman alpha radiation with a single scale height extending several radii from the planet establishes the presence of atomic hydrogen in the Mars exosphere.

INTRODUCTION

On July 31 and August 5, 1969, the first observations of the ultraviolet spectrum of the Mars upper atmosphere were made with ultraviolet spectrometers on board the Mariner 6 and 7 spacecraft. The principal emission features were quickly identified and reported in the literature (Barth et al., 1969). A continued examination of these ultraviolet observations has revealed that they are rich in spectral detail and contain sufficient altitude information to make possible the determination of the composition and structure of the Mars upper atmosphere.

The purpose of the present report is twofold: (1) to give the results of a detailed spectroscopic analysis of the data which lead to the identification of the principal mechanisms producing the upper atmosphere emissions, and (2) to present the intensities of individual spectral features as a function of altitude so that models of the Mars upper atmosphere may be constructed. A review of the techniques and

theory of the ultraviolet spectroscopy of planets (Barth, 1969) shows a number of the spectral emissions that were being sought in the Mariner 6 and 7 experiment.

INSTRUMENT

The Mariner 6 and 7 ultraviolet spectrometer consists of a 250 mm focal length Ebert-Fastie scanning monochromator, a 250 mm focal length off-axis telescope, and a two photomultiplier tube detector system (Pearce et al., 1971). The spectral range 1900 - 4300 Å was measured in the first order at 20 Å resolution with a bialkali photomultiplier tube and the spectral range 1100 - 2100 Å in the second order at 10 Å resolution with a cesium iodide photomultiplier tube. A complete spectral scan including both orders was completed every three seconds. Extensive light baffling was used to reject light from the bright disc of the planet while observing the upper atmosphere.

OBSERVATIONAL GEOMETRY

The spectral emissions from the upper atmosphere of Mars were observed by having the ultraviolet spectrometer look tangentially through the atmosphere as the spacecraft flew by the planet. Since the relative velocity of the spacecraft with respect to the planet was 7 km/sec, a complete spectral scan was obtained every 21 km as the effective observation point, i.e., the closest point of the tangential line of sight, moved deeper into the atmosphere. The ultraviolet spectrometers on each Mariner had the opportunity to view the atmosphere twice, once looking ahead, once looking sideways as each spacecraft flew by Mars making a total of four probes of the upper atmosphere. The geometry of the observations is shown in Figure 1. In the case of Mariner 6, the solar zenith angle of the effective observation point was 27° for the first limb crossing and 0° for the second. For Mariner 7, the first limb crossing had a solar zenith angle of 44° and the second 0°. In all cases, the observations were made at an instrument zenith angle of 90°.

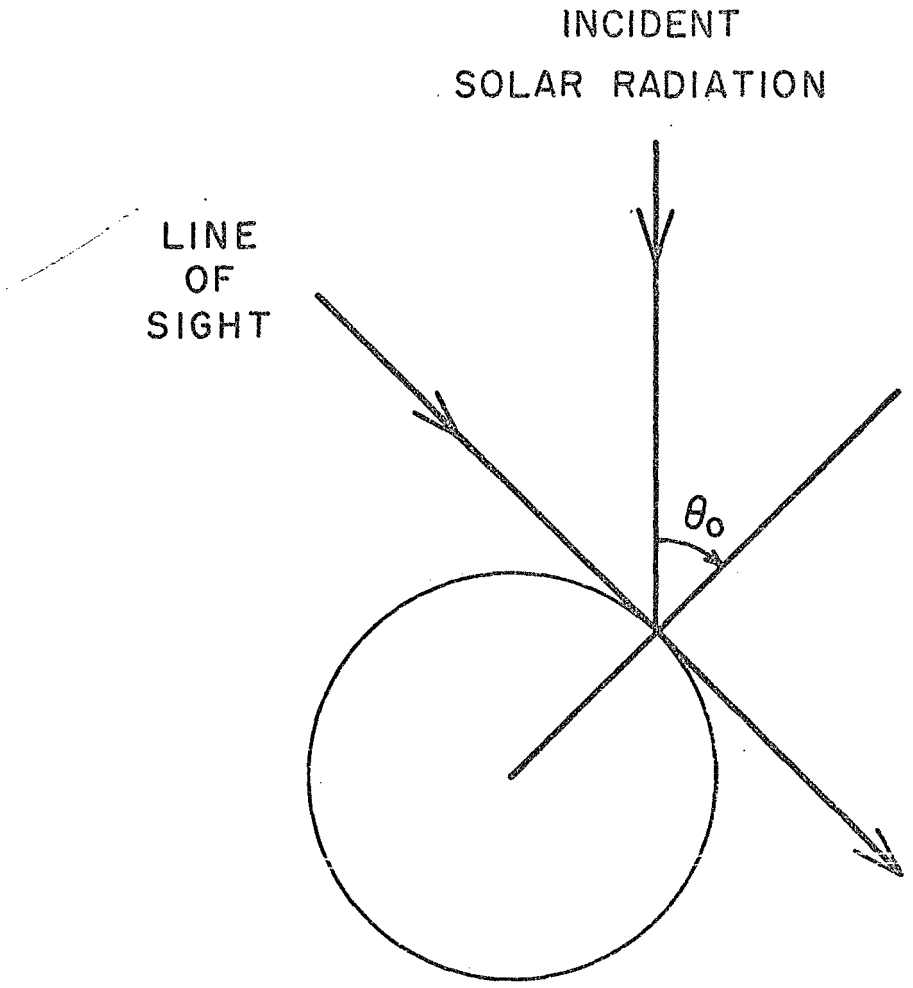

Fig. 1 Geometry of atmospheric limb observations. In all four limb crossings, the line of sight was perpendicular to a radius vector making the instrument zenith angle $\Theta = 90°$. The solar zenith angle Θ_o was 27° and 44° for the first limb crossings of Mariner 6 and 7, respectively, and 0° for both second limb crossings.

SPECTRUM

The ultraviolet spectrum of the upper atmosphere of Mars consists of the CO_2^+ $\tilde{A}\ ^2\Pi_u$ - $\tilde{X}\ ^2\Pi_g$ and $\tilde{B}\ ^2\Sigma_u^+$ - $\tilde{X}\ ^2\Pi_g$ bands, the CO $a\ ^3\Pi$ - $X\ ^1\Sigma$ Cameron and $A\ ^1\Pi$ - $X\ ^1\Sigma^+$ fourth positive bands, the CO^+ $B\ ^2\Sigma^+$ - $X\ ^2\Sigma^+$ first negative bands, the CI 1561 and 1657 Å lines, the OI 1304, 1356, and 2972 Å lines, and the HI 1216 Å Lyman alpha line. These spectral emission features are shown in the spectra in Figures 2 and 3. Figure 2 displays the Mars spectrum between 1900 and 4300 Å at 20 Å resolution, which was obtained while the instrument was observing the Mars atmosphere at an altitude between 160 and 180 km above the surface. Figure 3 shows the spectral interval between 1100 and 1800 Å at 10 Å resolution. This spectrum originated from the 140 to 160 km level of the Mars upper atmosphere. Both the long and short wavelength spectra that are displayed here are the result of summing four individual three-second spectral scans.

Fig. 2 Ultraviolet spectrum of the upper atmosphere of Mars, 1900 - 4000 Å, 20 Å resolution. Spectrum was obtained by observing the atmosphere tangentially at an altitude between 160 and 180 km. This spectrum was obtained from the sum of four individual observations.

Fig. 3 Ultraviolet spectrum of the upper atmosphere of Mars, 1100 - 1800 Å, 10 Å resolution. Spectrum was obtained by observing the atmosphere tangentially at an altitude between 140 and 160 km. This spectrum was obtained from the sum of four individual observations.

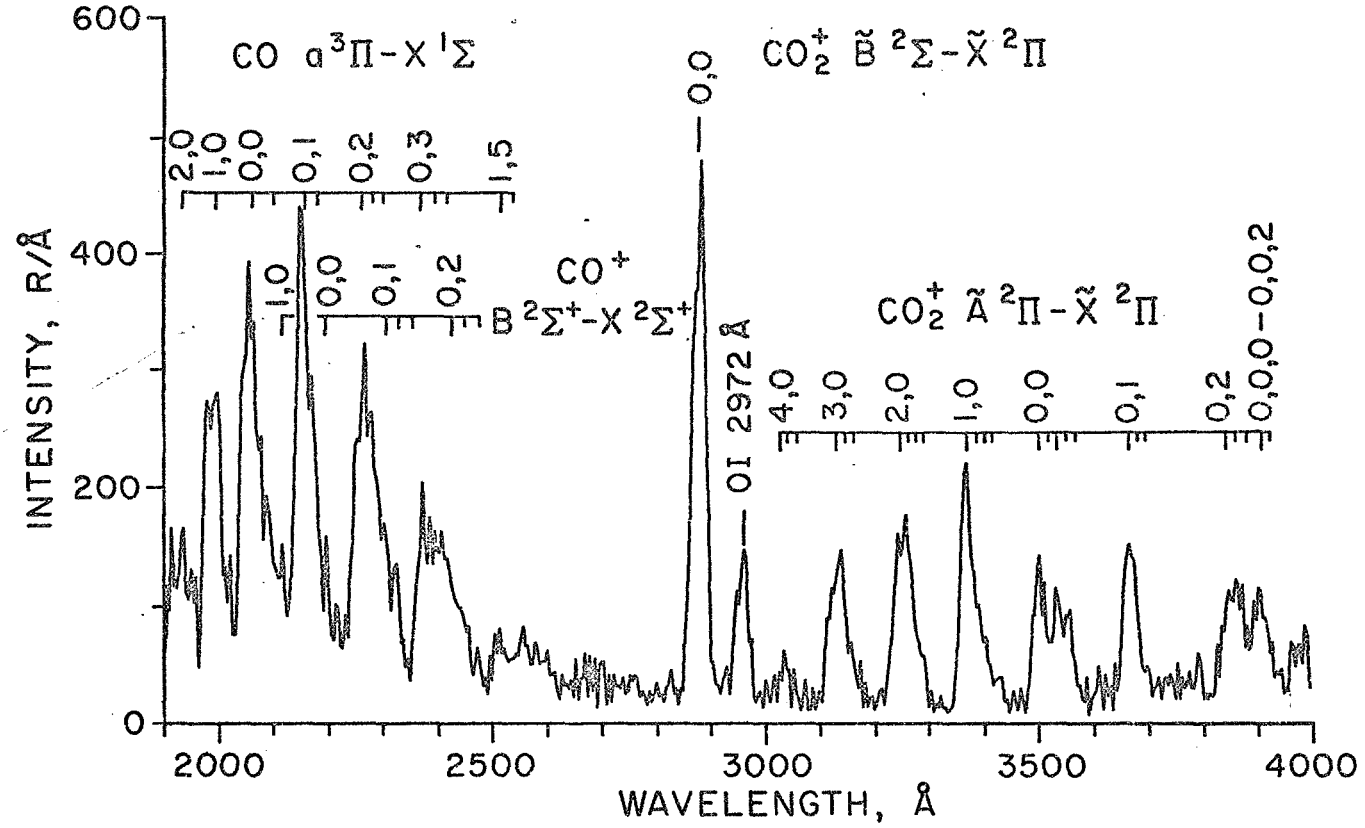
CO a³Π-X¹Σ
CO₂⁺ B̃ ²Σ-X̃ ²Π
0,0
2,0
1,0
0,0
0,1
0,2
0,3
1,5
CO⁺
B ²Σ⁺-X ²Σ⁺
1,0
0,0
0,1
0,2
OI 2972 Å
CO₂⁺ Ã ²Π-X̃ ²Π
4,0
3,0
2,0
1,0
0,0
0,1
0,2
0,0,0-0,0,2
INTENSITY, R/Å
WAVELENGTH, Å

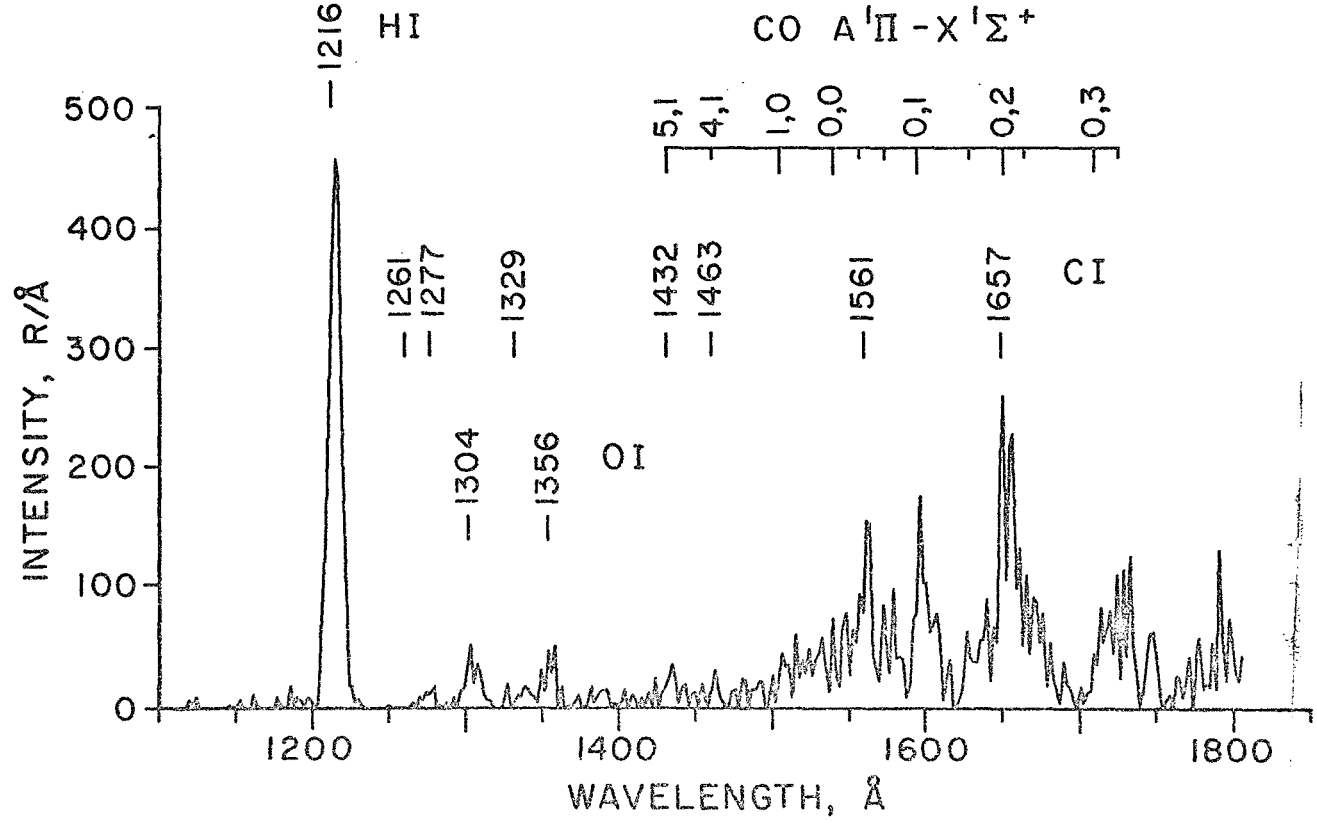
1216 HI
CO A¹Π-X¹Σ⁺
5,1
4,1
1,0
0,0
0,1
0,2
0,3
1261
1277
1329
1432
1463
1561
1657
CI
1304
1356
OI
INTENSITY, R/Å
WAVELENGTH, Å

EMISSION MECHANISMS

The B-X and A-X CO_2^+ bands may be produced in the Mars upper atmosphere by one or more of three mechanisms: (1) fluorescent scattering of solar radiation by carbon dioxide ions, (2) photoionization excitation of neutral carbon dioxide by extreme ultraviolet solar radiation, and (3) electron impact excitation of neutral carbon dioxide by the photoelectrons produced in the photoionization of the major constituents in the Mars atmosphere. These processes may be represented by the following set of equations which also lists the wavelength of the solar radiation or the energy of the electrons responsible for the excitation.

$$CO_2^+ (\tilde{X}\ ^2\Pi_g) + h\nu \rightarrow CO_2^+ (\tilde{B}\ ^2\Sigma_u^+) \qquad \lambda = 2890\ \text{Å}$$

$$CO_2^+ (\tilde{X}\ ^2\Pi_g) + h\nu \rightarrow CO_2^+ (\tilde{A}\ ^2\Pi_u) \qquad \lambda \leq 3507\ \text{Å}$$

$$CO_2 (\tilde{X}\ ^1\Sigma_g^+) + h\nu \rightarrow CO_2^+ (\tilde{B}\ ^2\Sigma_u^+) + e \qquad \lambda < 686\ \text{Å}$$

$$CO_2 (\tilde{X}\ ^1\Sigma_g^+) + h\nu \rightarrow CO_2^+ (\tilde{A}\ ^2\Pi_u) + e \qquad \lambda < 716\ \text{Å}$$

$$CO_2 (\tilde{X}\ ^1\Sigma_g^+) + e \rightarrow CO_2^+ (\tilde{B}\ ^2\Sigma_u^+) + 2e \qquad E > 18.1\ \text{ev}$$

$$CO_2 (\tilde{X}\ ^1\Sigma_g^+) + e \rightarrow CO_2^+ (\tilde{A}\ ^2\Pi_u) + 2e \qquad E > 17.3\ \text{ev}$$

Since the relative intensities between the two electronic transitions and among the extensive vibrational development in the A-X system contain information about the excitation mechanism, laboratory and theoretical studies were conducted for each of the three mechanisms. The spectra produced by the impact of 20 eV electrons on neutral carbon dioxide were found to be similar but not identical to the spectra produced by the impact of 584 Å photons on CO_2. At equivalent energies, the cross sections for the two processes were found to be nearly equal (Wauchop and Broida, 1971; Ajello, 1971). In analogy to the production of the N_2^+ 3914 Å band in the earth's atmosphere, photoionization excitation is a more likely source of excitation of the CO_2^+ bands in the Mars spectrum than photoelectron excitation, because a large number of photons are available for the photoionization excitation and because the threshold for electron impact excitation lies above the energy of most of the photoelectrons. A dayglow model calculation for a pure CO_2 - CO_2^+ atmos-

phere illustrates the dominance of the photoionization excitation (Dalgarno, Degges, and Stewart 1970). The photoionization excitation spectrum produced by 584 Å photons which was recorded in the laboratory by a Mariner ultraviolet spectrometer is shown in Figure 4. A comparison between it and the Mars spectrum in Figure 2 shows that the vibrational distribution in the A-X bands is not the same in the two spectra. For example, in the Mars spectrum the 0,0 band is more intense than the 2,2 where in the laboratory spectrum the reverse is true. When the laboratory spectrum was subtracted from the Mars spectrum, the bands at longer wavelengths which arise from the lowest vibrational levels were the most intense in the spectrum that remained. The emphasis on the lower vibrational levels is indicative of a spectrum produced by fluorescent scattering since the higher vibrational levels require shorter wavelength photons for excitation, and the solar spectrum falls off with decreasing wavelength

Fig. 4 Laboratory photoionization excitation spectrum of CO_2 produced with 584 Å photons.

Fig. 5 Theoretical fluorescent scattering spectrum for CO_2^+.

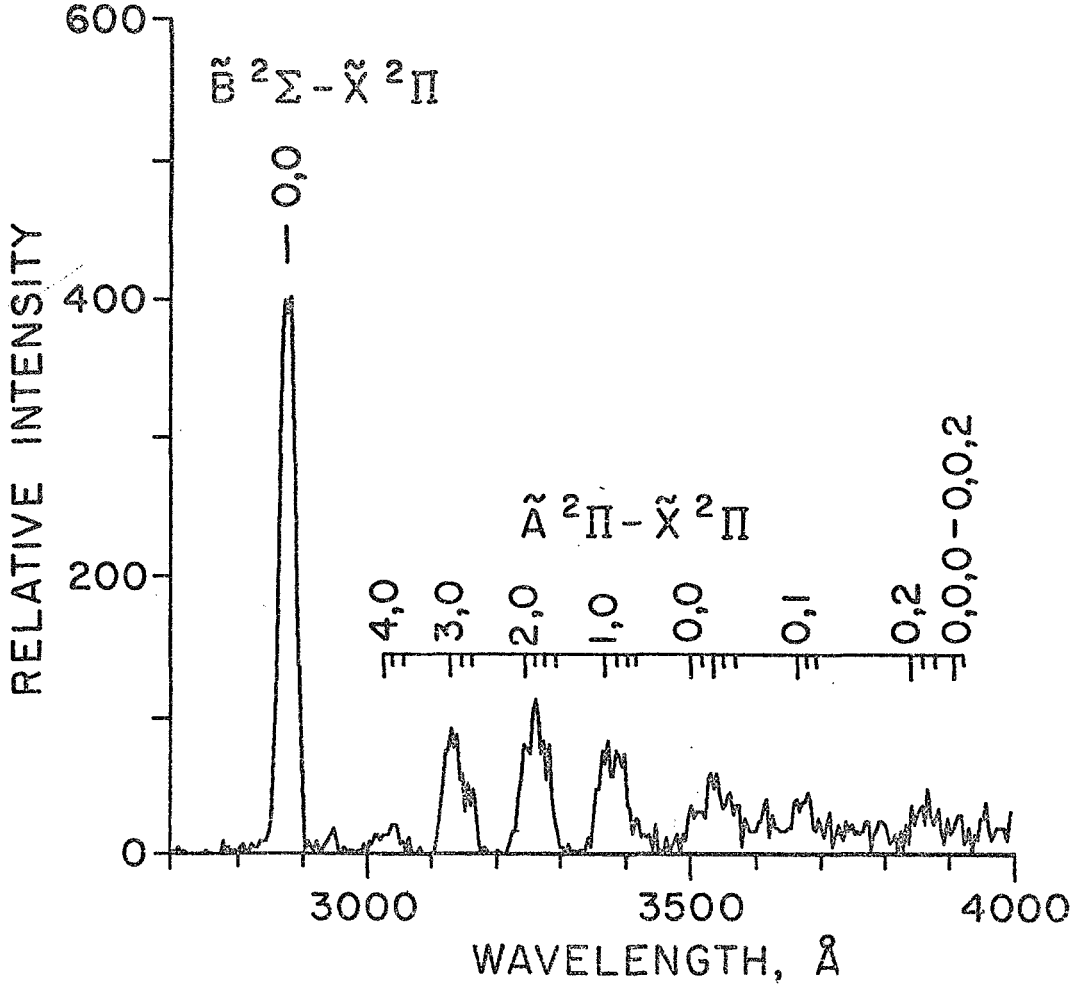
600
400
200
0
RELATIVE INTENSITY
$\tilde{B}\,^2\Sigma - \tilde{X}\,^2\Pi$
0,0
$\tilde{A}\,^2\Pi - \tilde{X}\,^2\Pi$
4,0
3,0
2,0
1,0
0,0
0,1
0,2
0,0,0-0,0,2
3000
3500
4000
WAVELENGTH, Å

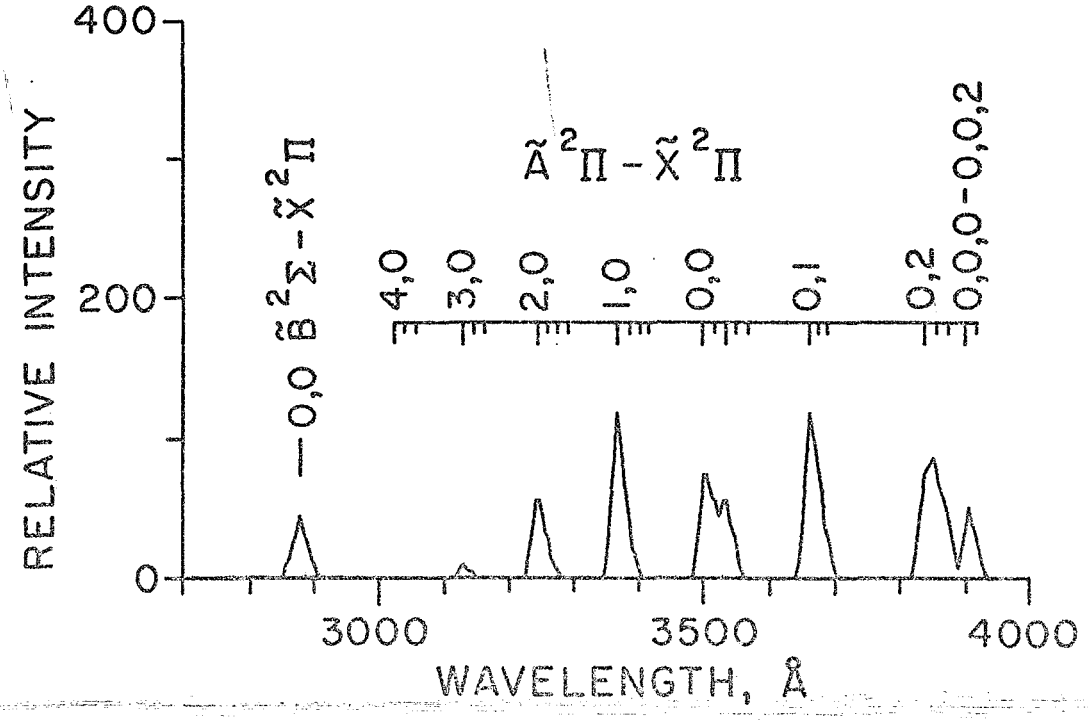
400
200
0
RELATIVE INTENSITY
0,0 $\tilde{B}\,^2\Sigma - \tilde{X}\,^2\Pi$
$\tilde{A}\,^2\Pi - \tilde{X}\,^2\Pi$
4,0
3,0
2,0
1,0
0,0
0,1
0,2
0,0,0-0,0,2
3000
3500
4000
WAVELENGTH, Å

in this part of the spectrum. A synthetic spectrum which shows the relative intensities expected from fluorescent scattering is plotted in Figure 5. This spectrum was calculated from the transition probabilities measured by Hesser (1968) and the branching ratios derived by Dalgarno and Degges (1970) from the work of Poulizac and Dufay (1967). The relative intensity of the (0,0,0 - 0,0,2) band was determined from the laboratory measurements of Wauchop and Broida (1971).

The two spectra, the photoionization excitation spectrum in Figure 4 and the fluorescent scattering spectrum in Figure 5, add up quantitatively to match the intensity distribution of the CO_2^+ B-X and A-X bands in the Mars spectrum. At the particular altitude where this Mars spectrum was observed, the B-X (0,0) band is produced 90% by photoionization excitation and 10% by fluorescent scattering. Photoionization excitation is the stronger source of the A-X band system, but individual bands such as the (0,0) are produced more

strongly by fluorescent scattering. Thus, this analysis shows how the Mars ultraviolet spectrum between 2800 and 4000 Å may be used to measure quantitatively the number of CO_2^+ ions in the Martian ionosphere, the number of CO_2 molecules at the same altitude, and the rate of photoionization occurring in the Martian upper atmosphere.

The CO a-X Cameron bands are the most intense emission in the Mars ultraviolet spectrum. They may be excited by: (1) the fluorescent scattering of solar radiation by CO molecules in the Mars upper atmosphere; (2) the photoelectron excitation of carbon monoxide; (3) the photodissociation excitation of CO_2 molecules in the Mars upper atmosphere; (4) the photoelectron excitation of carbon dioxide molecules to produce excited carbon monoxide molecules; and (5) the dissociative recombination of ionized carbon dioxide molecules. These excitation mechanisms are described by the following set of equations where the energy of the photoelectrons or

the wavelength of radiation responsible for the excitation is also listed.

$$CO\ (X\ ^1\Sigma^+) + h\nu \rightarrow CO\ (a\ ^3\Pi) \qquad \lambda \leq 2063\ \text{Å}$$

$$CO\ (X\ ^1\Sigma^+) + e \rightarrow CO\ (a\ ^3\Pi) + e \qquad E > 6.01\ \text{ev}$$

$$CO_2\ (\tilde{X}\ ^1\Sigma_g^+) + h\nu \rightarrow CO\ (a\ ^3\Pi) + O \qquad \lambda < 1082\ \text{Å}$$

$$CO_2\ (\tilde{X}\ ^1\Sigma_g^+) + e \rightarrow CO\ (a\ ^3\Pi) + O + e \qquad E > 11.5\ \text{ev}$$

$$CO_2^+\ (\tilde{X}\ ^2\Pi_g) + e \rightarrow CO\ (a\ ^3\Pi) + O$$

Since the vibrational distribution of the CO Cameron bands is not the same for all five mechanisms, the relative populations of the upper vibrational levels give a clue to the actual mechanism that is operating in the upper atmosphere of Mars. The vibrational distributions for fluorescent scattering and photoelectron excitation of carbon monoxide have been calculated previously (Barth, 1966, 1969). Both of these predicted spectra differ from the vibrational distribution of the Cameron bands in the Mars spectrum. In the fluorescent scattering spectrum, the vibrational population of the upper level falls off more rapidly than in the Mars spectrum.

In the photoelectron excitation spectrum, the (1,0) band is more intense than the (0,0) while in the Mars spectrum the reverse is true. These two mechanisms are also inadequate to account for the intensity of the Cameron bands quantitatively. The upper state of the Cameron bands, the a $^3\Pi$, is metastable; its lifetime has been measured to be 7.5 ± 2 milliseconds (Lawrence, 1971). Because of the small oscillator strength associated with this transition, an amount of carbon monoxide far in excess of the total number of molecules in the Mars upper atmosphere would be required to produce the intensity of the Cameron bands observed in the Mars spectrum from fluorescent scattering. A similar quantitative argument may be made against these bands being produced by the photoelectron excitation of carbon monoxide.

The vibrational distribution produced by the remaining three processes is less well known. In

fact, there is not yet experimental evidence that the Cameron bands are produced by photodissociation excitation or dissociative recombination while they have been produced by electron impact excitation. To investigate the vibrational populations further, the Cameron bands were produced in the laboratory by bombarding carbon dioxide at a pressure of 10^{-3} Torr with 20 eV electrons. The electron-excited spectrum which was recorded by a Mariner-type ultraviolet spectrometer is shown in Figure 6. The vibrational distribution of the Cameron bands in this laboratory source and the Mars ultraviolet spectrum is nearly the same. Using Franck-Condon factors calculated by Nicholls (1962) it was determined that the lowest vibrational level of the upper state was the most populated. Levels up through $v' = 6$ were observed with their populations dropping off relatively slowly with increasing vibrational number. When the identified Cameron bands were subtracted from the Mars ultraviolet

Fig. 6 Laboratory electron excitation spectrum of CO_2 produced with 20 eV electrons.

Fig. 7 Laboratory electron excitation spectrum of CO_2 produced with 50 eV electrons.

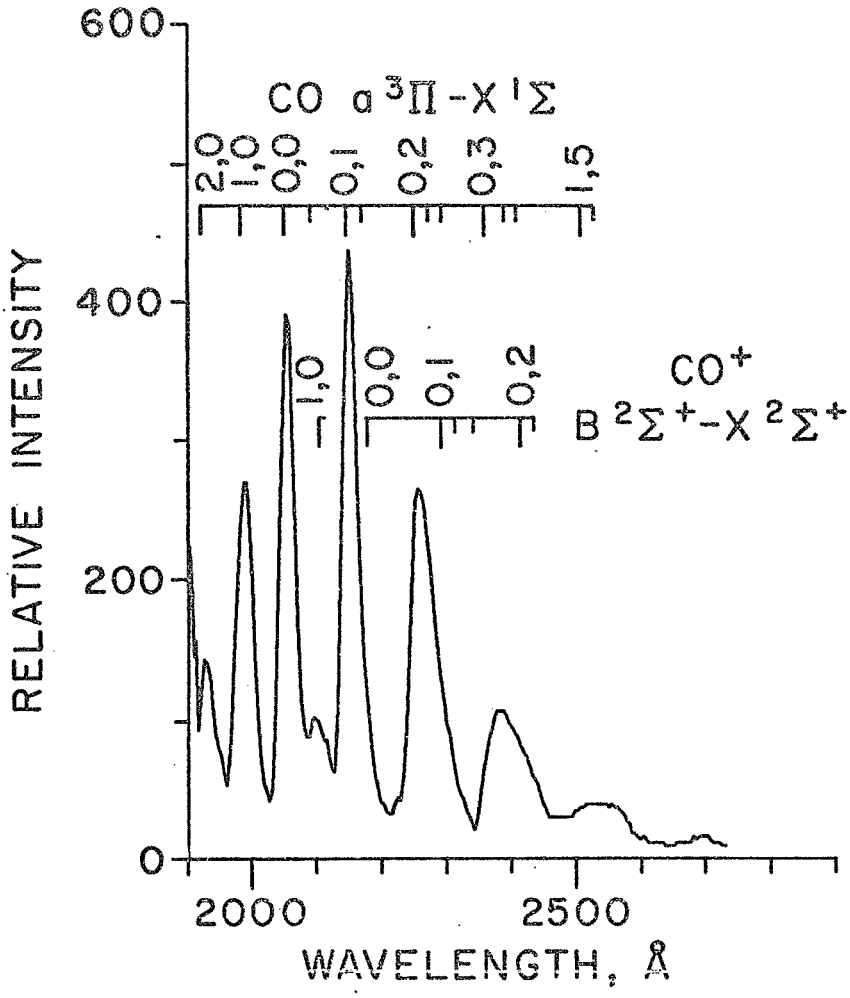
600
400
200
0
RELATIVE INTENSITY
CO a $^3\Pi$ - X $^1\Sigma$
2,0
1,0
0,0
0,1
0,2
0,3
1,5
1,0
0,0
0,1
0,2
CO$^+$
B $^2\Sigma^+$ - X $^2\Sigma^+$
2000
2500
WAVELENGTH, Å

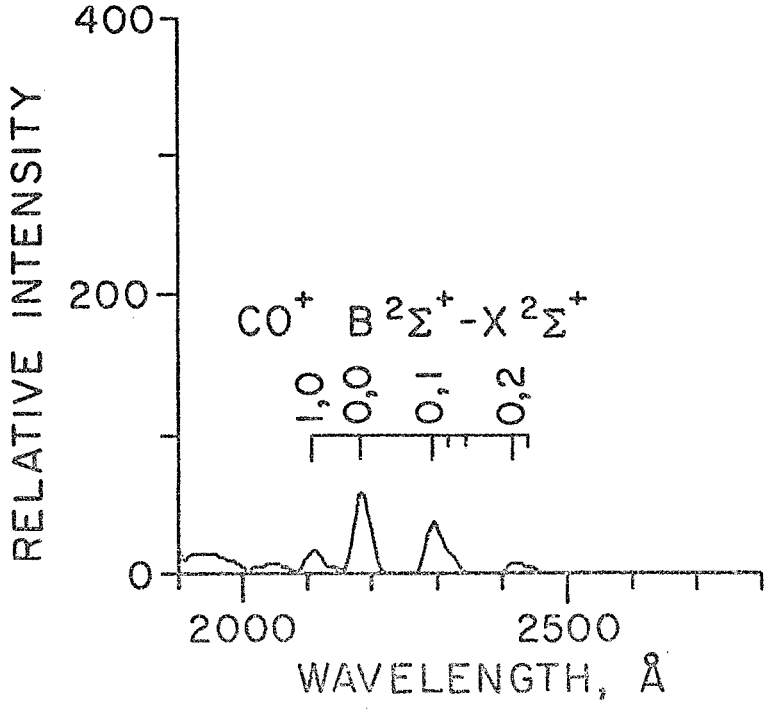
400
200
0
RELATIVE INTENSITY
CO$^+$ B $^2\Sigma^+$ - X $^2\Sigma^+$
1,0
0,0
0,1
0,2
2000
2500
WAVELENGTH, Å

spectrum with the aid of the Franck-Condon factors, some spectral features remained. These are identified as the CO^+ B $^2\Sigma$ - X $^2\Sigma$ first negative bands. They are also produced in the laboratory by the impact of electrons on carbon dioxide. A laboratory spectrum which emphasizes these bands is shown in Figure 7 as recorded by a Mariner-type spectrometer. In the figure, the amplitude of the first negative bands has been adjusted to match the intensity present in the Mars spectrum in Figure 2. First negative bands are also present in the laboratory spectrum in Figure 6. The relative populations of the vibrational levels of the CO a $^3\pi$ state and the CO^+ B $^2\Sigma$ state in the Mars spectrum are given in the Table.

On the basis of the laboratory experience with the CO_2^+ band systems where similar spectra are produced with similar cross sections by electrons and photons of equal energy, it may be expected that photodissociation excitation of carbon dioxide by extreme ultraviolet radiation will produce the

TABLE Vibrational Populations of the Upper States of the Cameron bands a $^3\Pi$ - X $^1\Sigma$, the first negative bands B $^2\Sigma$ - X $^2\Sigma$, and the fourth positive bands A $^1\Pi$ - X $^1\Sigma^+$ in the Mars spectrum.

Excited State	Relative Population
a $^3\Pi$, v' = 0	1.00
1	0.67
2	0.36
3	0.29
4	0.18
5	0.10
6	0.10
7	0.10
B $^2\Sigma$, v' = 0	1.00
1	0.90
2	0.21
A $^1\Pi$, v' = 0	1.00
1	0.77
2	0.46
3	0.32
4	0.17
5	0.15
6	0.14

Cameron bands with a vibrational distribution similar to that produced by electrons. If the cross sections for photon and electron impact are similar, then an argument analogous to the one used with the CO_2^+ bands would suggest that photodissociative excitation of carbon dioxide would be the dominant mechanism in the Mars upper atmosphere. If the electron impact dissociative excitation cross section is much larger than the photodissociative excitation cross section, then photoelectron excitation may be the dominant source of the Cameron bands.

The dissociative recombination of CO_2^+ is energetically capable of producing the Cameron bands with an extensive number of vibrational levels populated, but the laboratory experiment to measure radiation from this reaction has not been performed. However, with the CO_2^+ densities for the Mars ionosphere that are derived from the CO_2^+ A-X bands, and the recombination rate measured in the laboratory (Weller and Biondi, 1967), it does not appear that

sufficient recombinations can take place to produce the observed intensity even if all recombinations produce the Cameron bands.

The CO A-X fourth positive bands may be produced in the Mars upper atmosphere by the same five processes that are potential sources of the Cameron bands: (1) fluorescent scattering by CO, (2) photoelectron excitation of CO, (3) photodissociation excitation of CO_2, (4) photoelectron dissociative excitation of CO_2, and (5) dissociative recombination of CO_2^+. The following equations describe these mechanisms and the wavelengths of the solar radiation responsible for their excitation.

$$CO\ (X\ ^1\Sigma^+) + h\nu \rightarrow CO\ (A\ ^1\Pi) \qquad \lambda \leq 1545\ \text{Å}$$

$$CO\ (X\ ^1\Sigma^+) + e \rightarrow CO\ (A\ ^1\Pi) + e \qquad E > 8.02\ \text{ev}$$

$$CO_2\ (\tilde{X}\ ^1\Sigma^+) + h\nu \rightarrow CO\ (A\ ^1\Pi) + O\ (^3P) \qquad \lambda < 920\ \text{Å}$$

$$CO_2\ (\tilde{X}\ ^1\Sigma^+) + e \rightarrow CO\ (A\ ^1\Pi) + O\ (^3P) + e \qquad E > 13.5\ \text{ev}$$

$$CO_2^+\ (\tilde{X}\ ^2\Pi_g) + e \rightarrow CO\ (A\ ^1\Pi) + O\ (^3P)$$

In contrast to the Cameron bands, the first mechanism, the fluorescent scattering of solar

radiation by carbon monoxide molecules, cannot be eliminated on a quantitative basis. In fact, because of the large oscillator strength of the A-X transition, this band system is ideally suited to be a measure of the amount of carbon monoxide in the Mars upper atmosphere (Barth, 1969). However, as will be seen from the analysis of the vibrational distribution, the bulk of the excitation of the fourth positive band in the Mars spectrum cannot come from fluorescent scattering by CO molecules. A similar argument can be made against photoelectron excitation of CO being a strong contributor.

How the vibrational distribution of the fourth positive bands may be used to identify the source of excitation was explored using the techniques developed for the previous band systems; namely, the production of this band system in the laboratory by bombarding CO_2 with 20 eV electrons. The spectrum in Figure 8 which was obtained in the laboratory with a Mariner-type spectrometer shows

Fig. 8 Laboratory electron excitation spectrum of CO_2 produced with 20 eV electrons.

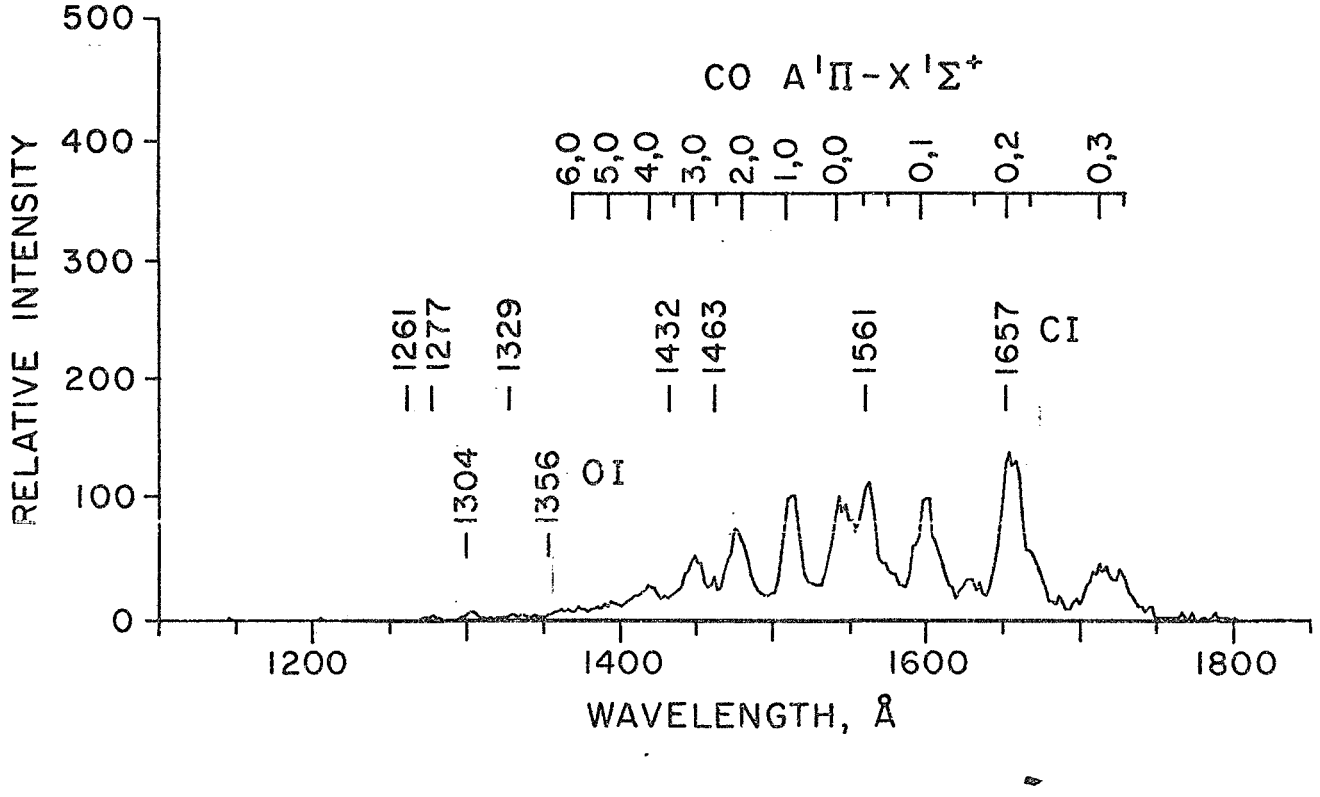
CO A¹Π-X¹Σ⁺
6,0
5,0
4,0
3,0
2,0
1,0
0,0
0,1
0,2
0,3
1261
1277
1329
1432
1463
1561
1657
CI
1304
1356
OI
RELATIVE INTENSITY
500
400
300
200
100
0
1200
1400
1600
1800
WAVELENGTH, Å

bands arising from vibrational levels from $v' = 0$ up to $v' = 6$. The lowest level has the greatest population, but all of the levels up through 6 are populated as well. When the laboratory spectrum is compared with the Mars spectrum in Figure 3, an analysis shows that the vibrational populations in the two sources are nearly the same although the spectra themselves have differences. What are missing in the Mars spectrum as compared with the laboratory one, are fourth positive bands whose lower vibrational level is the lowest vibrational level of the ground electronic state, the $v'' = 0$ level. The reason why they are missing must be that sufficient CO molecules are present in the Mars upper atmosphere so that self-absorption is taking place in transitions connected to the ground vibrational level.

The measured vibrational populations of the upper state of the fourth positive bands are also given in the Table. The population distribution in the Mars spectrum is different from the distri-

bution that would be produced by mechanisms (1) and (2) (fluorescent scattering and photoelectron excitation of CO) and thus, these data may be used to eliminate these mechanisms as principal contributors. Dissociative recombination of CO_2^+, mechanism 5, is also eliminated by these measured vibrational populations since this mechanism is energetically only able to excite the $v' = 0$ and 1 levels and the observed Mars spectra show substantial populations up through the $v' = 3$ level. This leaves only mechanisms 3 and 4, photodissociative excitation and photoelectron dissociative excitation of CO_2, as sources of the Mars fourth positive bands. No doubt both mechanisms are operating, but following the arguments given previously for the Cameron bands, namely, that in dissociative excitation processes, the excitation cross sections are approximately the same for photons or electrons of equal energy, the major source of fourth positive band excitation should be photodissociative excitation

because the number of photons that is available is greater than the number of photoelectrons.

When a synthetic spectrum of the fourth positive bands was subtracted from the Mars spectrum, emission lines from atomic carbon remained. From the positions of a number of the ultraviolet lines of CI which are marked in the Figure, it may be seen that there is a clear cut identification of the 1561 and 1657 Å lines. Carbon lines also appear in the laboratory spectrum produced by the impact of 20 eV electrons on CO_2 as can be seen in Figure 8. The most likely source of excitation of the carbon lines in the Mars spectrum is photodissociative excitation or photoelectron dissociative excitation of carbon dioxide. If there were free carbon atoms in the Martian atmosphere, the 1561 and 1657 Å lines could be produced by resonant scattering (Barth, 1969). In any case, the measured intensity of the carbon lines may be used to determine an upper limit to the number of carbon atoms present in the upper atmosphere.

The atomic oxygen lines at 1304, 1356 and 2972 Å may be produced in the Mars upper atmosphere by (1) resonant scattering of solar radiation by atomic oxygen, (2) photoelectron excitation of atomic oxygen, (3) photodissociative excitation of carbon dioxide, and (4) photoelectron dissociative excitation of carbon dioxide. Only the ^3P - ^3S transition that produces the 1302, 1304, 1306 Å triplet is an allowed transition and thus, is the only serious candidate for the resonant scattering mechanism. The ^3P - ^5S transition that produces the 1356, 1358 Å doublet and the ^3P - ^1S transition that produces the 2972 Å lines are forbidden transitions but may be produced by the photoelectron and photodissociation mechanisms. The atomic hydrogen 1216 Å Lyman alpha line may be excited by (1) resonant scattering of solar radiation by atomic hydrogen, or (2) photodissociative excitation of molecular hydrogen (Barth et al., 1968). Photoelectron excitation of either the atom or molecule is not significant because of the small frac-

tional abundance of either form of hydrogen in the Mars ionosphere. The most plausible first choice of excitation for the 1216 Å line is resonant scattering of solar Lyman alpha radiation.

ALTITUDE DETERMINATION

While the distance from the earth to the Mariner spacecraft flying by Mars could be measured to a fraction of a kilometer, (Anderson et al., 1970) it was not possible to determine the height above the surface of Mars of the tangential line of sight of the ultraviolet spectrometer to better than tens of kilometers from the spacecraft orientation. However, the distance between successive ultraviolet spectrometer measurements was determined to better than a kilometer since those measurements were dependent on the motion of the spacecraft. Thus, scale heights of particular emission features could be determined with sufficient accuracy to be useful in formulating atmospheric models.

It is possible, however, to determine a nominal altitude scale by assuming a simple atmospheric model and using the ultraviolet data themselves to determine the altitude scale (Stewart, 1971). The radio occultation experiment which measured the electron density in the Mars ionosphere determined that the maximum electron concentration occurred at an altitude of 135 km at a location where the solar zenith angle was 57° (Fjeldbo et al., 1970). Since this height measurement directly depended on the tracking of the spacecraft, it was possible to achieve an accuracy within 1 km. By assuming that the upper atmosphere is nearly pure carbon dioxide and that the maximum electron density occurs at the same altitude as the maximum rate of photoionization, it is possible to calculate that the total column density of CO_2 above 135 km is 4.2×10^{16} molecules cm^{-2}. As will be seen in the next section, the Cameron bands, besides being the most intense emission, were observed over the most extensive altitude range of

any of the ultraviolet emissions. Using carbon dioxide absorption coefficients and the model atmosphere, the location of a maximum in the Cameron band emission was calculated to be at 135 km assuming that photodissociation was the excitation mechanism. Since the observations were made edge-on through a spherical atmosphere, the maximum in the intensity distribution occurs ten km lower at 125 km. The altitude variations of the Cameron bands for each of the four limb crossings were then fitted to a calculation appropriate to an overhead sun even in the cases where the solar zenith angle was 27° and 44°. This procedure then established the altitude scale for all of the upper atmosphere emissions.

ALTITUDE VARIATION

Observations that were made on each of the two limb crossings on Mariners 6 and 7 yielded the variation with altitude of the spectral emissions from the 100 km level of the upper atmosphere to as far up as the particular constituent could be detected.

For the airglow that originates with the carbon dioxide molecule, the emissions extend upward to 220 km, near the top of the thermosphere. Atomic oxygen and atomic hydrogen emissions are present in the exosphere, as well, extending outward to an altitude of 700 km for atomic oxygen and to a planetocentric distance of 25,000 km for atomic hydrogen.

The intensity of the CO_2 B-X and A-X bands as viewed tangentially through the atmosphere is shown in Figure 9. The scale height of the A-X bands is greater than that of the B-X bands since, as the spectroscopic analysis has shown, fluorescent scattering by CO_2^+ makes a major contribution to the A-X emissions while the photoionization excitation of CO_2 is the major source of the B-X bands. The scale height of the ion is usually greater than that of the neutral species for either photochemical or diffusive equilibrium. The two different scale heights for the two mechanisms may be seen more clearly in Figure 10 where the intensity of two bands

of the A-X transition that originate from different upper vibrational levels are plotted. The (2,0) band originating principally from photoionization excitation has a smaller scale height than the (0,1) which originates predominantly from fluorescent scattering.

The most intense emission in the ultraviolet portion of the spectrum, the CO a-X Cameron bands, is plotted as a function of altitude in Figure 11. Since this emission originates from photodissociation or photoelectron dissociative excitation of CO_2, the altitude profile of the emission is proportional at high altitudes to the density distribution of neutral carbon dioxide. The maximum intensity that is measured near 125 km is over 600 kR or 6×10^{11} photons cm^{-2} sec^{-1} of airglow between 1903 and 2843 Å consisting principally of the Cameron bands although there is a small contribution from the CO^+ first negative bands. When this emission rate is adjusted to give the zenith rate for this emission, the value

Fig. 9 Slant intensity of the CO_2^+ B-X and A-X band systems as a function of altitude.

Fig. 10 Slant intensity of the CO_2^+ A-X (2,0) and (0.1) bands as a function of altitude. Note discontinuity in the intensity scale.

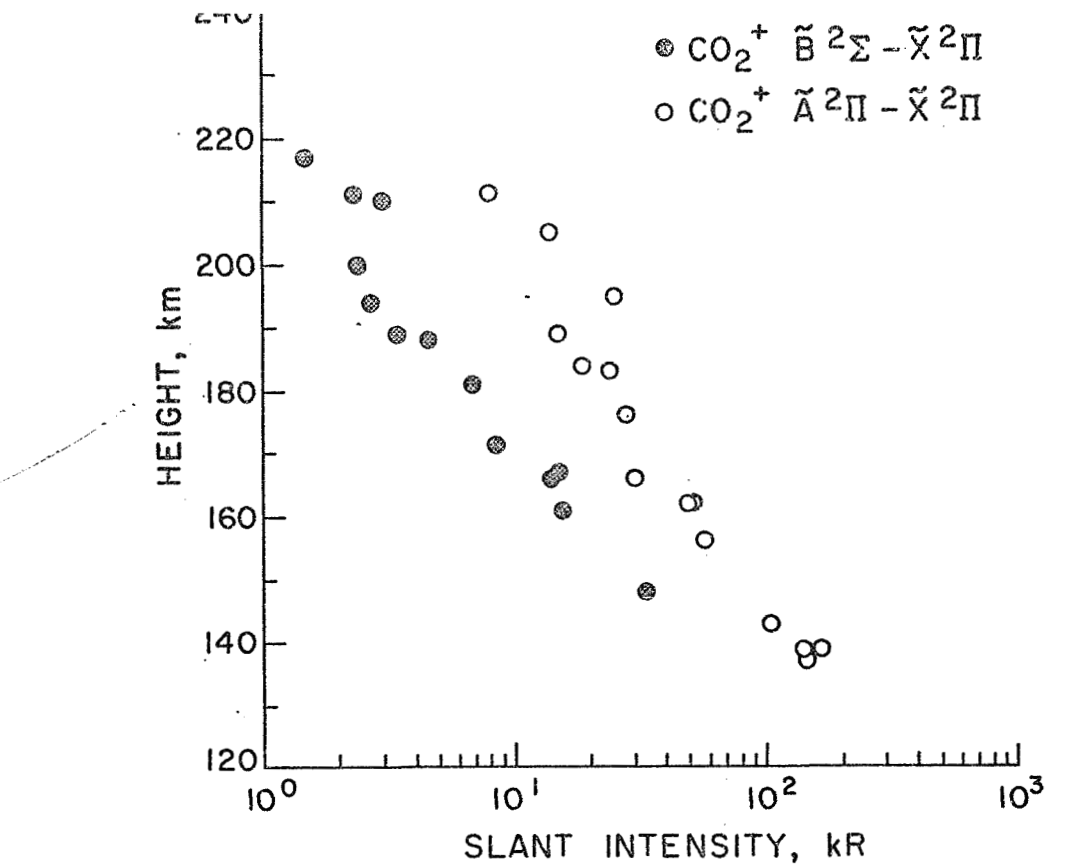
CO_2^+ $\tilde{B}\,^2\Sigma - \tilde{X}\,^2\Pi$
CO_2^+ $\tilde{A}\,^2\Pi - \tilde{X}\,^2\Pi$
HEIGHT, km
220
200
180
160
140
120
10^0
10^1
10^2
10^3
SLANT INTENSITY, kR

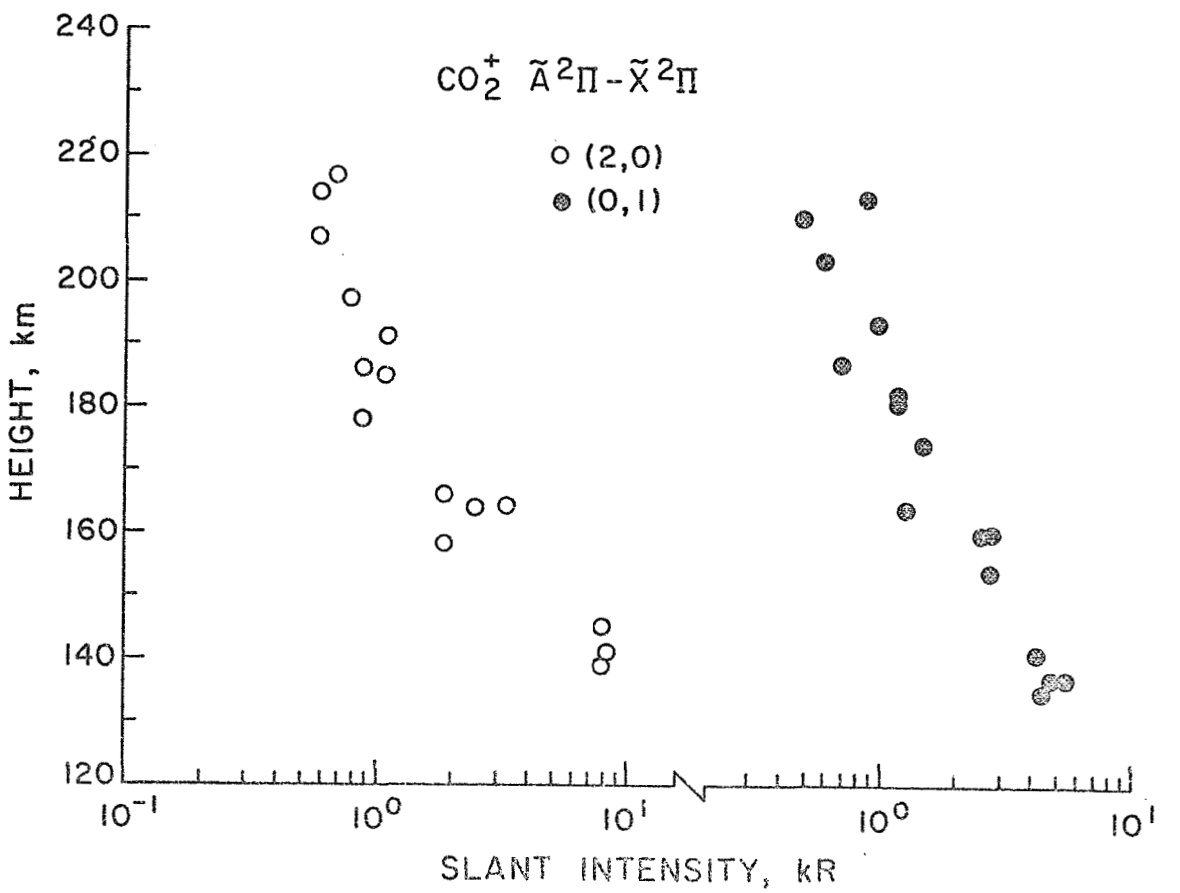
CO_2^+ $\tilde{A}\,^2\Pi - \tilde{X}\,^2\Pi$
(2,0)
(0,1)
HEIGHT, km
240
220
200
180
160
140
120
10^{-1}
10^0
10^1
10^0
10^1
SLANT INTENSITY, kR

obtained is 20 kR or 2 x 10^{10} photons cm^{-2} sec^{-1}. This is equal to a sizeable fraction of the total number of photons cm^{-2} sec^{-1} in the solar flux at wavelengths shorter than 1082 Å, the photodissociative threshold for the Cameron bands.

The altitude variation of the CO A-X fourth positive bands was determined by fitting a synthetic spectrum including the (v',0) bands to the Mars spectra normalizing on the (v',v'' ≠ 0) bands. The emission rate of the atomic carbon lines was determined by subtracting the synthetic spectra from the Mars spectra. The slant intensities as a function of altitude of the fourth positive bands and the CI 1657 Å line are plotted as a function of altitude in Figure 12. These emissions reach a maximum near 145 km because below that altitude the airglow at this wavelength is absorbed by CO_2. At higher altitudes, the fourth positive bands also follow the same scale height as the Cameron bands, which is the neutral carbon dioxide scale height. The altitude

Fig. 11 Slant intensity of the CO a-X Cameron Bands and the OI 2972 Å line as a function of altitude.

Fig. 12 Slant intensity of the CO A-X fourth positive bands, the CI 1657 Å line, and the OI 1356 Å line as a function of atltitude.

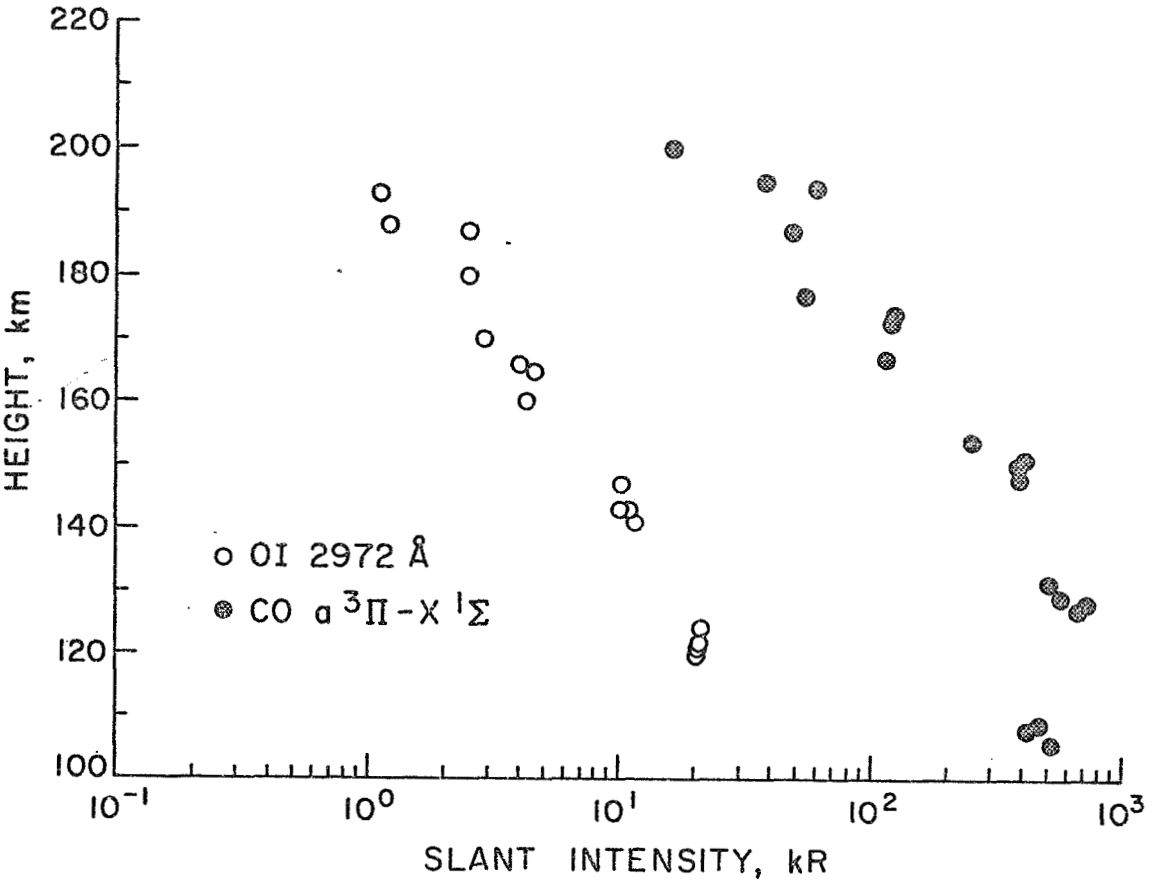
220
200
180
160
140
120
100
HEIGHT, km
o OI 2972 Å
● CO a $^3\Pi$ - X $^1\Sigma$
10^{-1}
10^0
10^1
10^2
10^3
SLANT INTENSITY, kR

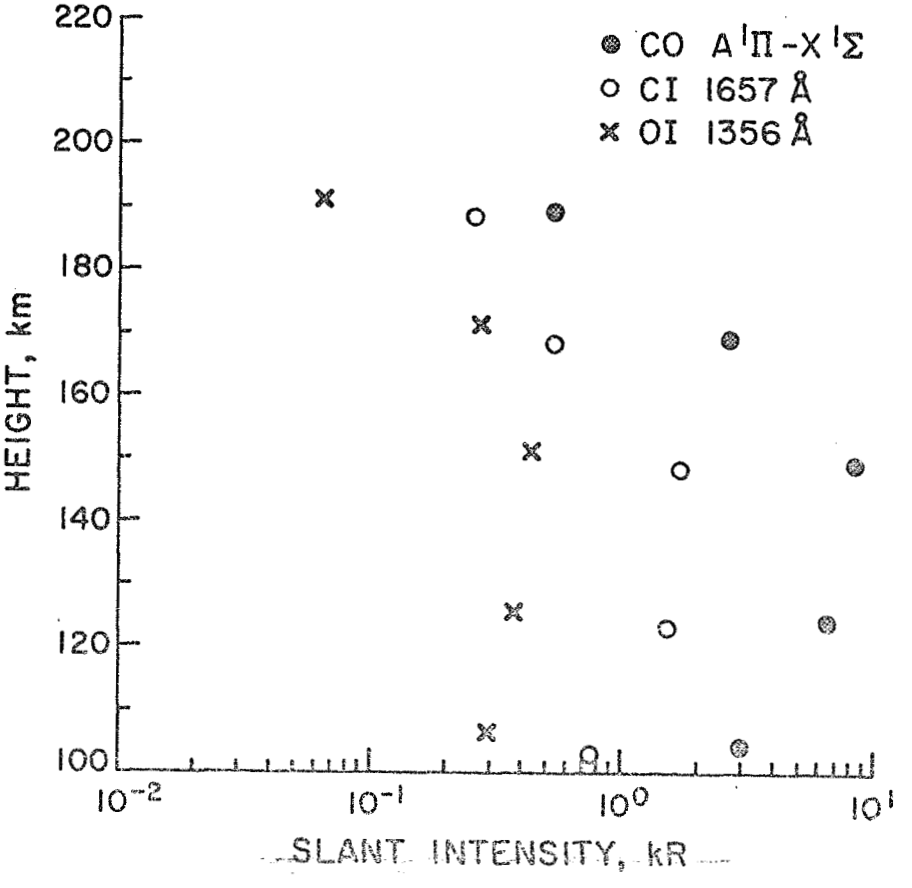
220
200
180
160
140
120
100
HEIGHT, km
● CO A $^1\Pi$ - X $^1\Sigma$
o CI 1657 Å
× OI 1356 Å
10^{-2}
10^{-1}
10^0
10^1
SLANT INTENSITY, kR

profile of the atomic carbon line also follows this scale height for the point at the highest altitude measured whose deviation may or may not be real. The most likely altitude dependence of this line is the same as that of the other emissions arising from dissociative excitation processes of CO_2.

The slant intensity of the 2972 Å atomic oxygen line is shown in Figure 11 as a function of altitude. Since its altitude dependence clearly follows that of the CO a-X Cameron bands that are plotted in the same figure, the excitation mechanism for the line most probably is the same as for the Cameron bands; namely, the dissociation of CO_2 by photons or electrons. Above the altitude where the maximum intensity occurs, about 125 km, the 2972 Å intensity follows the carbon dioxide altitude distribution. In Figure 12, the 1356 Å atomic oxygen has the same altitude dependence as the carbon monoxide bands suggesting that this line also is produced from CO_2 in a dissociative excitation process.

Fig. 13 Slant intensity of the OI 1304 Å line as a function of altitude for the two limb crossings of Mariner 6.

Fig. 14 Slant intensity of the OI 1304 Å line as a function of altitude for the two limb crossings of Mariner 7.

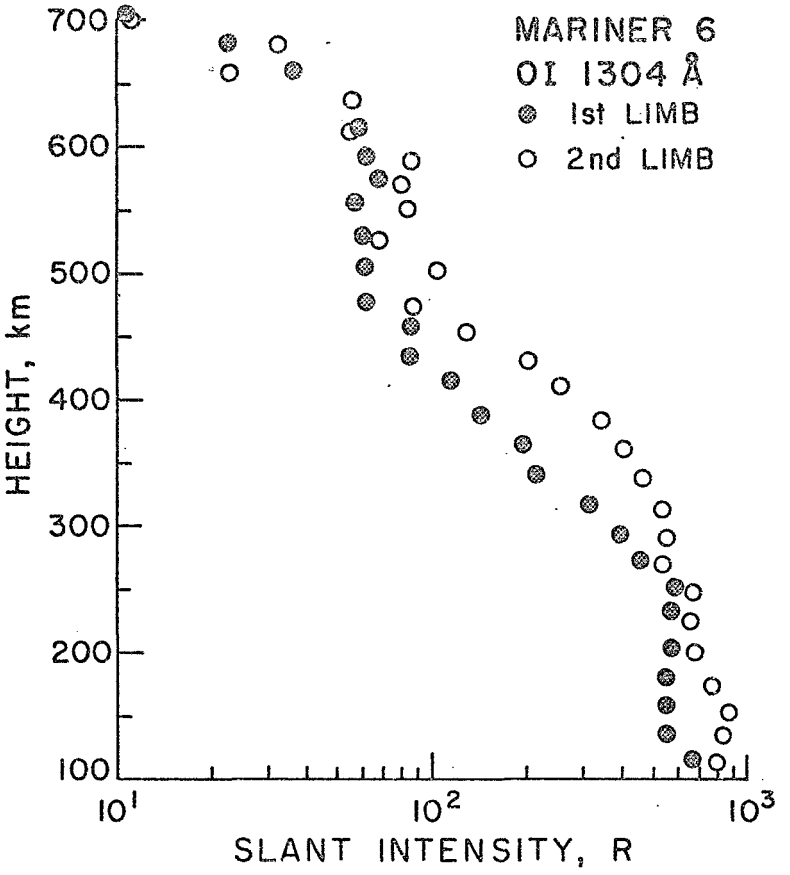
MARINER 6
OI 1304 Å
1st LIMB
2nd LIMB
HEIGHT, km
700
600
500
400
300
200
100
10^1
10^2
10^3
SLANT INTENSITY, R

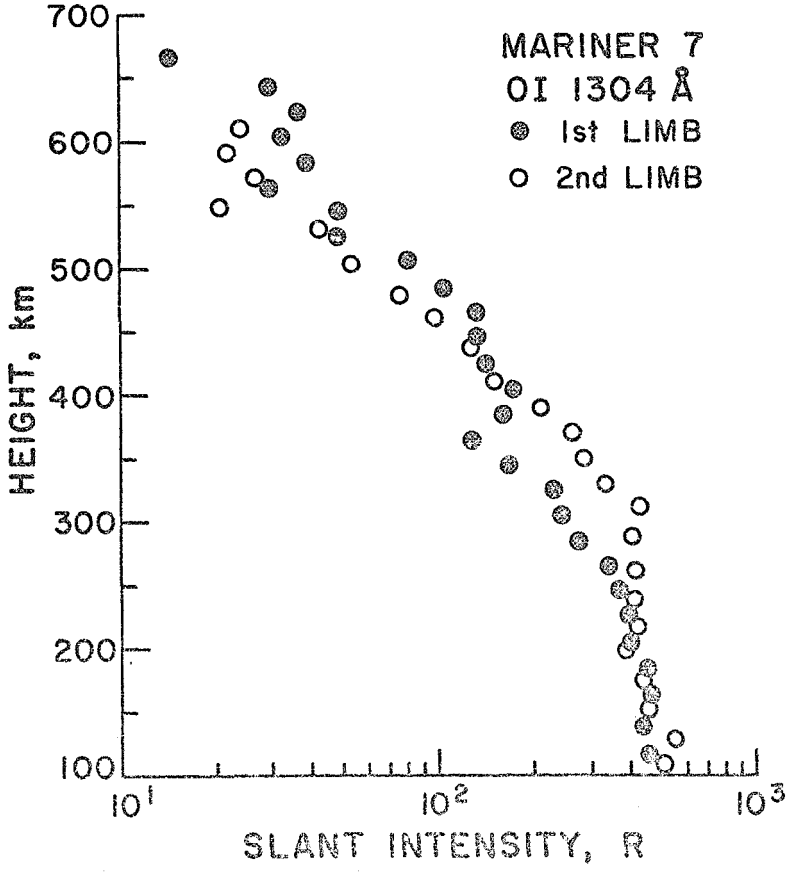
MARINER 7
OI 1304 Å
1st LIMB
2nd LIMB
HEIGHT, km
700
600
500
400
300
200
100
10^1
10^2
10^3
SLANT INTENSITY, R

The altitude distribution of the atomic oxygen 1304 Å line is quite different from that of the other atomic oxygen emissions indicating that its excitation process is different from those producing the 1356 and 2972 Å lines. In Figures 13 and 14, the slant intensity of the 1304 Å emission is plotted as a function of altitude for the two limb crossings for each of the two spacecraft. This atomic oxygen line was detectable all the way up to 700 km in contrast to the altitude range of all of the other spectral emissions described so far which terminate at approximately 240 km. Such an altitude distribution indicates that the 1304 Å emission originates from a process that excites atomic oxygen itself. This is true certainly above 240 km and may be true over the entire observed altitude range. Examination of the data indicates that there is not a single well-defined scale height, but instead an altitude variation that suggests that there are two excitation processes, one with a maximum at very high altitudes

Fig. 15 Slant intensity of the HI 1216 Å Lyman alpha line as a function of planetocentric distance for Mariner 6. A value of 300 R for the Lyman alpha sky background has been subtracted.

Fig. 16 Slant intensity of the HI 1216 Å Lyman alpha line as a function of planetocentric distance for Mariner 7. A value of 300 R for the Lyman alpha sky background has been subtracted.

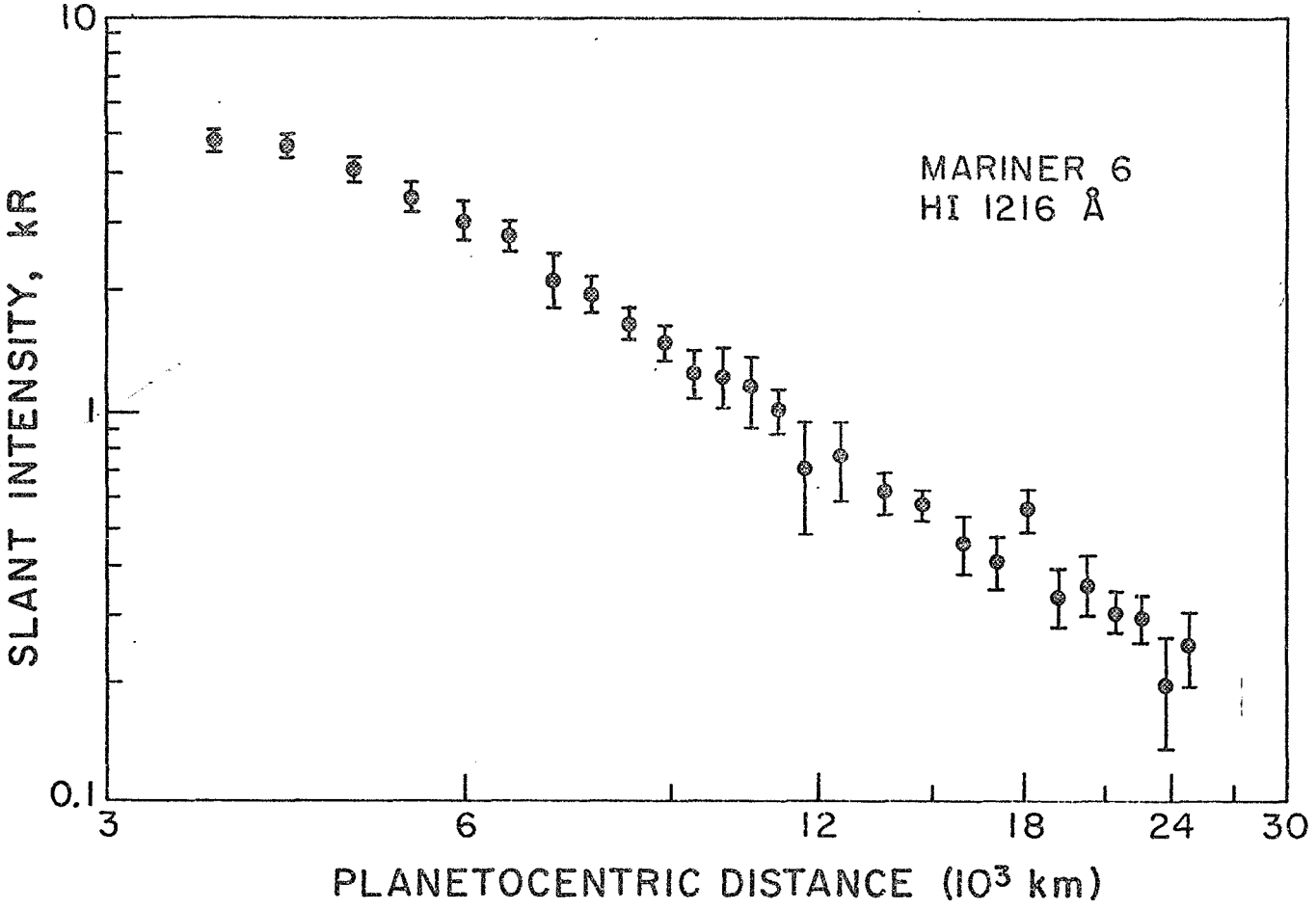
MARINER 6
HI 1216 Å
SLANT INTENSITY, kR
10
1
0.1
3
6
12
18
24
30
PLANETOCENTRIC DISTANCE (10³ km)

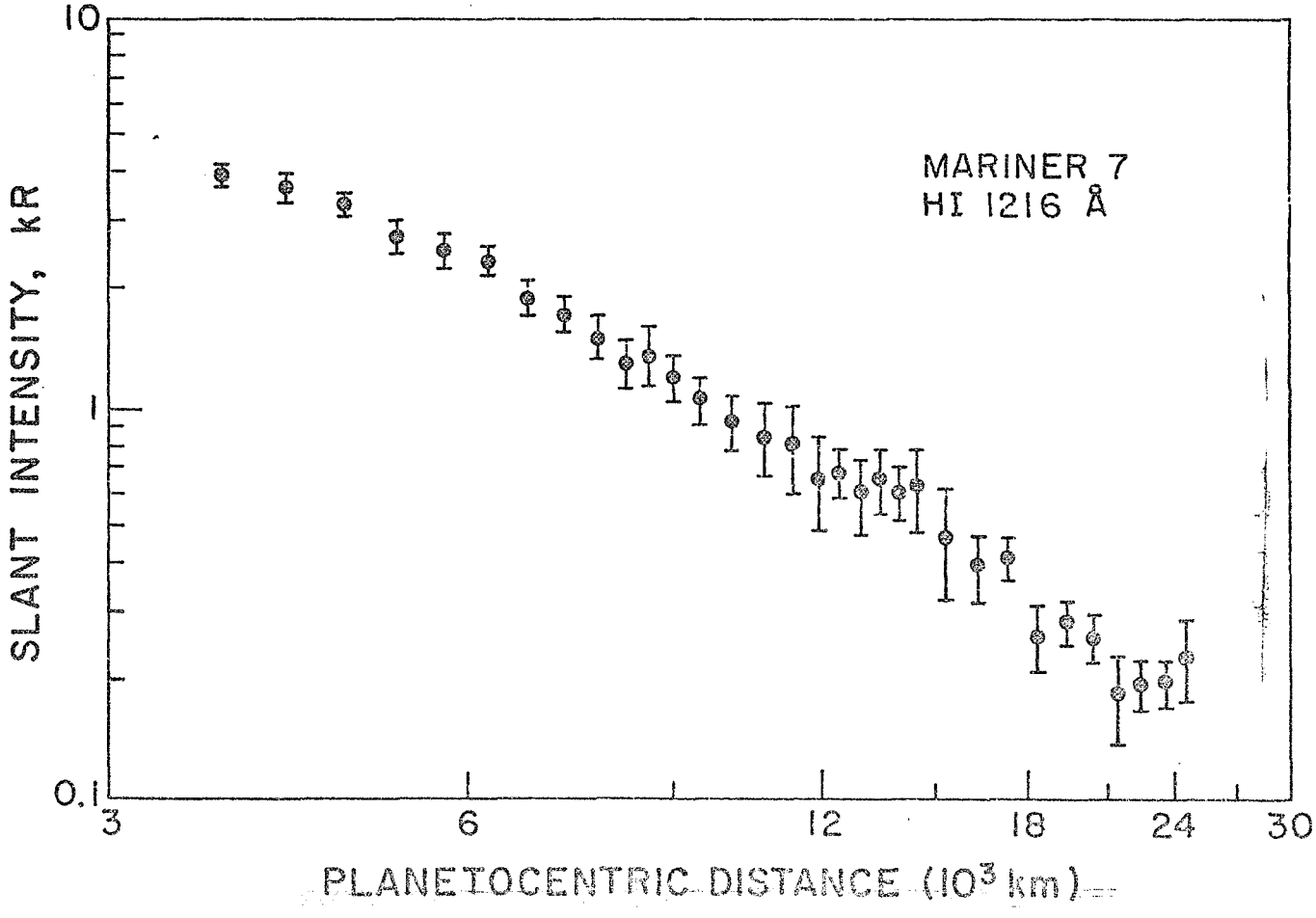
MARINER 7
HI 1216 Å
SLANT INTENSITY, kR
10
1
0.1
3
6
12
18
24
30
PLANETOCENTRIC DISTANCE (10³ km)

in the 500 to 700 km range and the other with a maximum in the 100 to 300 km range. In analogy with the excitation processes producing the 1304 Å line in the earth's airglow, the high altitude excitation process on Mars must be the resonant scattering of solar radiation by atomic oxygen and the low altitude source, the photoelectron excitation of atomic oxygen. Photon or electron impact dissociative excitation of carbon dioxide may also contribute to the low altitude source.

Lyman alpha radiation was observed all the way out to more than 20,000 km above the surface of Mars. The slant intensity as a function of the distance from the center of the planet is shown in Figure 15 for Mariner 6 and Figure 16 for Mariner 7. A value of 300 R for the Lyman alpha sky background has been subtracted from the observed intensity in preparing these figures (Barth, 1970). The existence of a single scale height in this altitude distribution suggests the most plausible excitation mechanism to

be the resonant scattering of solar radiation by atomic hydrogen in the Mars exosphere.

DISCUSSION

While the data that have been presented contain sufficient information to determine the structure and composition of the upper atmosphere of Mars, quantitative interpretation of the spectral emissions and the construction of model atmospheres is left for future publications. However, a qualitative examination of these ultraviolet observations allows several important conclusions to be drawn concerning the Mars upper atmosphere. First, with the exception of the HI 1216 Å, OI 1304 Å lines and a portion of the CO_2^+ A-X bands, all of the emissions may be and probably are produced by action of solar photons and photoelectrons on carbon dioxide. Second, with these same exceptions, all of the scale heights are the same and are small. These two conclusions mean that the upper atmosphere is essentially undissociated and cold. Third, since atomic oxygen emissions are

observed above 250 km, some dissociation of the CO_2 has occurred. Fourth, since part of the CO_2^+ A-X emission is attributed to fluorescent scattering, ionized carbon dioxide is a constituent of Mars' ionosphere, but not necessarily the major constituent. Lastly, the presence of atomic hydrogen in the exosphere of a planet with such a comparatively low gravitational field, means that there must be a source of dissociation of a hydrogen-bearing molecule such as water that is currently operating in the Mars atmosphere.

ACKNOWLEDGEMENT

The ability to achieve four limb crossings with a well-aligned slit from two spacecraft moving at 7 km/sec relative to Mars was the result of the highly cooperative, responsible interaction of the several scientists conducting experiments on the spacecraft, and the Mariner project staff. The principals were R. B. Leighton and B. C. Murray of the California Institute of Technoogy, the television experiment; G. C. Pimentel and K. C. Herr of the University of California at Berkeley, the infrared spectrometer experiment; G. Neugebauer and G. Münch of the California Institute of Technology, the infrared radiometer experiment; A. J. Kliore of the Jet Propulsion Laboratory, the radio occultation experiment; and H. M. Schurmeier, A. G. Herriman, and C. E. Kohlhase, the Mariner project staff. This work was supported by the National Aeronautics and Space Administration.

REFERENCES

Anderson, J. D., L. Efron and S. K. Wong, Martian Mass and Earth-Moon Mass Ratio from Coherent S-Band Tracking of Mariners 6 and 7, Science, 167, 277, 1970.

Ajello, J. M., Emission Cross Sections of CO_2 by Electron Impact in the Interval of 1260 Å to 4500 Å: Part II, J. Chem. Phys., 00, 0000, 1971.

Barth, C. A., The Ultraviolet Spectroscopy of Planets in The Middle Ultraviolet: Its Science and Technology, edited by A. E. S. Green, John Wiley & Sons, Inc., New York, 1966.

Barth, C. A., Planetary Ultraviolet Spectroscopy, Applied Optics, 8, 1295, 1969.

Barth, C. A., Mariner 6 Measurements of the Lyman-alpha Sky Background, Astrophys. J. Letters, 161, L181, 1970.

Barth, C. A., W. G. Fastie, C. W. Hord, J. B. Pearce, K. K. Kelly, A. I. Stewart, G. E. Thomas, G. P. Anderson and O. F. Raper, Mariner 6: Ultraviolet Spectrum of Mars Upper Atmosphere, Science, 165, 1004, 1969.

Barth, C. A., L. Wallace and J. B. Pearce, Mariner 5 Measurement of Lyman-alpha Radiation near Venus, J. Geophys. Res., 73, 2541, 1968.

Dalgarno, A., T. C. Degges and A. I. Stewart, Mariner 6: Origin of Mars Ionized Carbon Dioxide Ultraviolet Spectrum, Science, 167, 1490, 1970.

Dalgarno, A., and T. C. Degges, CO_2^+ Dayglow on Mars and Venus, Proceedings of IAU Symposium 40, Marfa, Texas, 1970.

Fjeldbo, G., A. Kliore and B. Seidel, The Mariner 1969 Occultation Measurements of the Upper Atmosphere of Mars, Radio Science, 5, 381, 1970.

Hesser, J. E., Absolute Transition Probabilities in Ultraviolet Molecular Spectra, J. Chem. Phys., 48, 2518, 1968.

Hord, C. W., C. A. Barth and J. B. Pearce, Ultraviolet Spectroscopy Experiment for Mariner Mars 1971, Icarus, 12, 63, 1970.

Lawrence, G. M., Quenching and Radiation Rates of CO ($a^3\pi$), Chem. Phys. Letters, 00, 000, 1971.

Nicholls, R. W., Laboratory Astrophysics, J. Quant. Spectrosc. Radiat. Transfer, 2, 433, 1962.

Pearce, J. B., K. A. Gause, E. F. Mackey, K. K. Kelly, W. G. Fastie and C. A. Barth, The Mariner 6 and 7 Ultraviolet Spectrometers, Applied Optics, 10, 000, 1971.

Poulizac, M. C., and M. Dufay, An Evaluation of CO_2^+ $^2\Pi_u \rightarrow {}^2\Pi_g$ Vibrational Transition Probabilities, Astrophys. Letters, 1, 17, 1967.

Stewart, A. I., Interpretation of some results of the Mariner 6 and 7 Ultraviolet Spectrometer Results, J. Geophys. Res., 76, 000, 1971.

Wauchop, T. S., and H. P. Broida, Cross Sections for the Production of Fluorescence of CO_2^+ in the Photoionization of CO_2 by 58.4 NM Radiation, J. Geophys. Res., 76, 21, 1971.

Weller, C. A., and M. A. Biondi, Measurements of Dissociative Recombination of CO_2^+ Ions with Electrons, Phys. Rev. Letters, 19, 52, 1967.

APPENDIX A

The slant intensities of the various emission features as a function of altitude are given in tabular form in this appendix. Table A1 lists the intensities for the CO_2^+ bands, the B-X band, the A-X band system, the A-X (2,0) band, and the A-X (0,1) band; Table A2 the CO a-X band system and the OI 2972 Å line; Table A3 the CO A-X band system, the OI 1356 Å line, and the CI 1657 Å line; and Table A4 the OI 1304 Å line. In all cases, the slant intensity which is given in kilorayleighs is the apparent column emission rate that is observed by viewing the spherical atmosphere from the outside, perpendicular to a radius vector. A kilorayleigh is 10^9 photons per second from a square centimeter column. It is equal to 4π times the apparent surface brightness of the atmosphere in 10^9 photons sec^{-1} cm^{-2} $ster^{-1}$.

For emissions at wavelengths longer than 2800 Å, a substantial background has been subtracted from the spectral data. The origin of this background is the

Table A1 Slant intensities of the CO_2^+ B-X band, the CO_2^+ A-X band system, the A-X (2,0) band, and the A-X (0,0) band as a function of altitude for the four limb crossings.

TABLE A1

	CO_2^+ B-X		CO_2^+ A-X		A-X 2,0		A-X 0,1	
	Altitude		Altitude		Altitude		Altitude	
	Km	kR	Km	kR	Km	kR	Km	kR
Mariner 6 First Limb Crossing	217	1.5	211	8.	214	.6	210	.5
	194	2.7	189	15.	191	1.1	187	.7
	171	8.5	166	30.	168	1.9	164	1.3
	148	>33.8	143	104.	145	8.1	141	4.3
Mariner 6 Second Limb Crossing	211	2.3	184	19.	186	.9	182	1.2
	189	3.4	162	51.	164	3.3	160	2.8
	167	15.4	139	>142.	141	8.4	137	4.8
Mariner 7 First Limb Crossing	-	-	-	-	217	.7	213	.9
	200	2.4	195	25.	197	.8	193	1.0
	181	6.9	176	28.	178	.9	174	1.5
	161	15.5	156	57.	158	1.9	154	2.8
	-	-	137	>146.	139	8.0	135	4.5
Mariner 7 Second Limb Crossing	210	3.0	205	14.	207	.6	203	.6
	188	4.6	183	24.	185	1.1	181	1.2
	166	14.3	162	49.	164	2.5	160	2.6
			139	>165.			137	5.5

Table A2 Slant intensities of the CO a-X band system and the OI 2972 Å line as a function of altitude for the four limb crossings.

TABLE A2

	CO		OI	
	Altitude	a-X	Altitude	2972 Å
	km	kR	km	kR
Mariner 6 First Limb Crossing	200	16.	193	1.1
	177	55.	170	2.9
	154	251.	147	10.2
	131	511.	124	21.0
	108	420.	-	-
Mariner 6 Second Limb Crossing	195	38.	188	1.2
	173	111.	166	4.0
	150	380.	143	10.3
	127	673.	120	>20.0
Mariner 7 First Limb Crossing	187	48.	180	2.5
	167	116.	160	4.3
	148	388.	141	11.6
	129	567.	122	21.5
	109	465.	-	-
Mariner 7 Second Limb Crossing	194	60.	187	2.5
	173	123.	165	4.6
	151	409.	143	11.0
	128	712.	121	20.6
	106	526.	-	-

Table A3 Slant intensities of the CO A-X band system, the OI 1356 Å line and the CI 1657 Å line as a function of altitude. The intensities for the four limb crossings have been averaged and are given as a function of the average altitude.

TABLE A3

Altitude km	CO A-X kR	OI 1356 Å kR	CI 1657 Å kR
200	.6	.1	.3
175	2.7	.3	.5
150	8.6	.4	1.7
125	6.9	.4	1.5
100	3.0	.3	.8

Table A4 Slant intensities of the 1304 Å line as a function of altitude for the four limb crossings. The intensities have been derived from a running five-point average where the altitude is that of the central point.

TABLE A 4

MARINER 6				MARINER 7			
First Limb Crossing		Second Limb Crossing		First Limb Crossing		Second Limb Crossing	
Altitude	OI 1304 Å	Altitude	OI 1304 Å	Altitude	OI 1304 Å	Altitude	OI 1304 Å
km	R	km	R	km	R	km	R
704	11	700	11	684	3	682	3
681	23	677	3	664	15	660	8
659	37	655	23	644	28	638	3
636	54	632	56	624	36	616	24
614	59	610	55	604	32	594	21
591	63	587	87	585	39	572	27
568	68	564	80	565	29	550	20
545	58	542	86	545	48	528	43
523	61	519	69	525	48	505	52
500	62	496	103	505	81	484	76
477	63	473	89	486	104	462	99
454	88	450	130	466	132	440	130
432	86	428	205	446	132	418	152
409	116	405	254	426	142	395	211
387	142	383	344	406	175	373	259
364	200	360	410	387	162	351	292
341	212	337	473	367	127	329	331
319	328	315	540	347	168	307	438
296	395	292	561	327	232	285	403
274	460	270	558	307	247	263	414
251	588	247	679	287	278	241	410
228	582	224	676	267	344	219	421
205	579	202	693	248	370	197	382
183	570	179	781	229	399	175	439
160	574	156	897	209	410	153	455
137	562	133	830	190	453	131	558
114	650	110	800	170	469	109	507
				151	427		
				131	460		
				111	427		

off-axis response of the instrument to the light from the bright disc of the planet. The spectral character of the disc is known from Mariner measurements that were made subsequent to the atmospheric limb observations and consists of the Fraunhofer spectrum of reflected sunlight. The intensities that are listed assume that the emission is uniform over the 0°.23 x 2°.3 field of view of the instrument and that the slit is aligned tangentially with the spherical atmosphere. Corrections for these assumptions can be made using the analytic formalism given in a discussion of the geometry of planetary spacecraft observations (Hord et al., 1970). For the two limb crossings each for Mariners 6 and 7, the slant range to the point where the line of sight was perpendicular to the radius vector was 7600, 6000, 8900, and 6200 km, respectively, and in all cases the slit was aligned tangentially within 3°.

For the spectral range above 1900 Å, the slant intensity of the emission features is given for each

individual limb crossing, while for those emission features below 1900 Å, except for the 1304 Å line, the slant intensities for the four limb crossings are averaged and the altitude given is the average altitude for the four observations. Because of the large number of data points, the Lyman alpha 1216 Å data are not given in tabular form but are available, along with the rest of these data, from the National Space Science Data Center.

Possible errors in the measured intensity of the Mars upper atmosphere spectral emissions may result from four causes: (1) the absolute calibration of the spectral response of the instrument, (2) the subtraction of the background produced by the off-axis response of the instrument, (3) the elimination of impulsive noise generated by the photomultiplier tubes, and (4) the subtraction of the electronic offset produced by imbalance in the amplifier circuits. The method of calibration and the estimate of the calibration errors are given in the instrument paper

(Pearce et al., 1971). Because of a lack of photometric standards for wavelengths less than 3000 Å, systematic errors in the calibration may be discovered in the future as standards are developed and adopted. For this same reason, the measured values of solar flux, which are used in conjunction with the planetary airglow data to determine upper atmosphere densities, may also be revised. However, the relative change in intensity with altitude, which is used to determine scale heights, will not be affected by changes in the absolute standards.

The three remaining causes, the subtraction of off-axis response, photomultiplier noise, and electronic off-set, are susceptible to subjective judgement in the reduction process. The subtraction processes has the largest effect on the data at high altitudes where the intensity is small and at low altitudes where the background is large. The errors involved in the subtraction process do affect the variation of intensity with altitude. These errors

may best be evaluated by a repetition of the reduction process which is possible by using the data available through the National Space Science Data Center.

For all of the emissions other than the 1216 Å Lyman alpha line, there were relatively few measurements made over the critical altitude region and an evaluation of the statistical variation of the measurements was not possible. However, for the Lyman alpha measurements, where the scale height is very large compared to the altitude interval between measurements, the root mean square variation which was determined for groups of fifty measurements, is given in Figures 15 and 16.